Dynamic Magnetorheological Damper for Orthotic Tremor Suppression

Biomedical Engineering and Technology
Mechatronics/MEMS/NEMS/Robotics/Automation

Presentation Format: Full Paper

Co-Author:
David Case
dcase@lyle.smu.edu

Presenting-Author:
Behzad Taheri
btaheri@lyle.smu.edu

Corresponding Author:
Edmond Richer, Ph.D.
richer@lyle.smu.edu

Department of Mechanical Engineering
Bobby B. Lyle School of Engineering
Southern Methodist University
PO BOX 750337, Dallas, TX 75275-0337
214-768-3059 Fax 214-768-1473

Dynamic Magnetorheological Damper for Orthotic Tremor Suppression

David Case, Behzad Taheri, and Edmond Richer

***Abstract*—This paper explores the design methodology and effectiveness of small-scale magnetorheological dampers (MRDs) in applications that require rapidly variable damping. Previously applications of MRDs have been chiefly limited to vehicle shock absorbers and seismic vibration attenuators. There has been recent biomedical interest in active-damping technology, particularly in the field of rehabilitation robotics. The topic at hand is the feasibility of developing MRDs that would be functionally and dimensionally adequate for actuation of an upper limb tremor suppression orthosis. A nonlinear Bingham plastic model is used to determine the MRD's functional characteristics, and experimental data is presented to validate the mathematical model. In addition, the dynamic response of the damper to step input signals and its bandwidth were estimated to explore its potential use in applications that require variable force at relatively high frequencies. A finite element analysis of the magnetic field within the damper was performed, resulting in an optimized design.**

***Index Terms*—Magnetic liquids; medical robotics; tremor suppression, orthotics.**

I. Introduction

A. Tremor and Current Clinical Treatment

TREMOR is one of the most common neurological disorders among adults [1], and it is clinically described as a rhythmical, involuntary oscillatory movement of a body part produced by reciprocally innervated antagonist muscles. It can be divided into two primary categories of movement disorders: resting and action (or essential) tremor [2]. Resting tremor, most commonly associated with Parkinson's disease, arises after a brief period of non-use of the target muscle or muscle group. While not particularly debilitating in and of itself, resting tremor can be the cause of severe social embarrassment. In contrast, action tremor becomes apparent during muscle use. The tremor typically manifests at a frequency in the range of 3 – 12 Hz and can be particularly debilitating to fine motor skills, that are required for the majority of daily activities [3]. Many patients complain of social embarrassment, and some have been driven to career changes.

Current treatments for various action tremors include a collection of prescription drugs and, in especially debilitating or non-responsive cases, neurosurgery. Symptomatic drugs typically prescribed for tremor (Propranalol, Primidone, botulinum toxin, and Levidopa to name a few) may cause the patient to experience excessive drowsiness, nausea, ataxia, confusion, blurred vision, fatigue, and even muscle paralysis, and hallucinations. Deep brain stimulation and stereotactic thalamotomy are invasive surgical options that involve controlled lesions or electrode placement in the brain, respectively. They have been linked with permanent complications, paresthesia, dysarthria, speech impediment, and even stroke and hemiparesis [4], [5]. Essential tremor and Parkinson's disease are degenerative conditions. Thus, while the administration of drugs, stereotactic thalamotomy, or thalamic deep brain stimulation is often initially effective in controlling tremor motion, none of these treatments guarantees a permanent solution [2], [3].

D. Case, B. Taheri, and E. Richer are with the Department of Mechanical Engineering, SMU, Dallas, TX 75205, USA; e-mail: ericher@smu.edu.

Manuscript submitted March 10, 2011

B. Tremor Orthoses

Due to the severe side effects and possible complications of current clinical treatments for action and resting tremor, many researchers recognized the necessity of a less-invasive alternative, the attenuation of tremor at the musculo-skeletal level. Sanes, LeWitt, and Mauritz reported that the application of viscous damping and inertia loads using brushless DC motors, "suppressed the (local) tremor nearly linearly" in the wrists of five patients experiencing various types of action tremors [6].

The "Controlled Energy Dissipation Orthosis" (CEDO), a 3 degrees of freedom (DOF) wheelchair-mounted device developed by MIT, functioned by applying resistive loads via magnetic particle brakes to a cuff attached to the patient's wrist. The second generation device, "Modulated Energy Dissipation Manipulator" (MEDM), allowed the wrist-cuff six degrees of freedom in three-dimensional space. While less restrictive to general motion, it was larger than the CEDO and non-portable. During evaluation of both devices, "the application of viscous damping loads was demonstrated to reduce tremor severity" [7]. Since no single set of damping parameters was observed to be most effective in attenuating tremor for all of the patients tested, the investigators concluded that the identification of individualized optimal damping levels is required.

The "viscous beam" orthosis, from the University of California Davis, was designed to attenuate tremor via viscous damping along the flexion and extension of the wrist. The device proved successful in principle, but its fixed damping rate induced inconsistent degree of functional success between patients [8].

An orthosis acting on the same general principle was created in the course of the European "Dynamically Responsive Intervention for Tremor Suppression" (DRIFTS) project, with the noted difference of employing a magnetorheological fluid. The design allowed tuning of the damping properties to optimize performance and was less restrictive to general motion. It allowed adduction/abduction and pronation/suppination and added viscous damping to flexion/extension of the wrist [9],

[10]. The "Wearable Orthosis for Tremor Assessment and Suppression" (WOTAS) was the final product of the DRIFTS project. This device was designed to be minimally restrictive to natural movement and capable of monitoring and suppressing tremor, employing both active and passive strategies [11]–[13]. The orthosis proved functionally successful in reducing the amplitude of the patients' tremor by as much as 90%, though there were some complaints on the aesthetic drawbacks of the device, and the investigators stressed the necessity of further reducing its size and weight [14], [15].

The main challenge for the design and construction of an effective, minimally intrusive, portable tremor canceling orthosis is the availability of compact, powerful, light, direct drive actuators and dampers. Thus, it is necessary to develop novel actuators/dampers that satisfy the power/force requirements for tremor cancelation, and have a sufficiently small profile and weight to be either hidden or easily ignored. In addition, to minimize interference with voluntary motion and avoid discomfort, they should exhibit the least amount of resistance force when back driven. None of the existing actuators combine all the desired characteristics. While electrical motors are easily powered by batteries and can be effectively controlled using relatively simple algorithms they cannot provide high force, low mechanical impedance actuation. Magnetorheological dampers excel at creating energy efficient variable damping forces but have relatively high mechanical impedance due to high viscosity of the fluid.

In this paper, a small scale MRD was designed using a mathematical model that considers the real annular geometry of the damper. Two sets of experiments, one quasi-static and the other dynamic, were conducted in order to validate the mathematical model and the applicability of MRDs for tremor suppression. Finite element analysis was performed to evaluate the magnetic field produced within the damper and examine potential improvements in its configuration.

II. Magnetoreological Fluids

A magnetorheological fluid (MRF) consists of a suspension of microscopic magnetizable particles in a non-magnetic carrier medium, usually a synthetic oil or water. In the absence of a magnetic field, the fluid behaves in a roughly Newtonian manner. When a magnetic field is applied, the microscopic particles suspended in the fluid form chains along the magnetic flux lines, changing the fluid's rheology (Fig. 1). The fluid exhibits a yield stress if flow occurs perpendicular to the magnetic flux lines, the properties of the fluid becoming non-isotropic. Thus, when a magnetic field is applied the MRFs behave similarly to a Bingham plastic.

Since the observed yield stress is directly related to the intensity of the magnetic field, MRFs seem ideally suited for use in a low-power tunable damper. Variable resistance through the use of MR fluids is a strategy currently being used commercially in vehicle shock absorbers and seismic vibration dampers for civic structures. In the field of human-machine interaction, particularly that of wearable robotics, high strength-to-weight ratio actuators are required to maximize assistive and rehabilitative potential [16]. MR-based

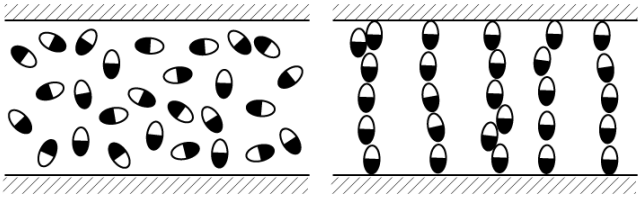

(a) (b)

Fig. 1. Particle arrangement in the absence (a) and presence (b) of magnetic flux across the elements

actuators can potentially achieve these high ratios and have the additional advantages of rapid response time and high fidelity control [17], [18]. These characteristics allow MRF dampers to be customized to the individual needs of a patient, as well as adjust the damping factor if the severity of the condition changes.

III. General Damper Design

With the intent of minimizing the profile of a tremor-suppression orthosis, the proposed design incorporates a series of linear dampers/actuators acting roughly in parallel to the muscles of the forearm. Dampers of the general design proposed here would be mounted above the dorsal and radial surfaces of the forearm, with the shafts connected to the hand using articulated linkages and an orthotic glove. Thus, a direct-drive mechanism for applying torque at the transverse and dorsopalmar axes of the wrist is formed. The palmar and ulnar surfaces would be unobstructed, allowing proximal movement and functionality at a desk.

In an attempt to balance efficiency with ease of manufacturing, a piston/cylinder design was adopted for the dampers. A copper coil wound about the middle section of the piston head creates the magnetic field in the annular gap between the piston and cylinder (Fig. 2). Both the cylinder wall and the piston head are machined from magnetically permeable material to close the magnetic circuit and direct the magnetic flux lines normal to the piston/cylinder gap.

DRIFTS project researchers measured the biomechanical characteristics of tremorous movement at each joint in the arms of 33 patients, providing the necessary torque characteristics for the actuators of a tremor-suppression orthosis [18]. The mean values of torque measured in the wrist are summarized in Table I. Considering a moment arm of 3 cm,

TABLE I
Torque Measurements At The Wrist

Movement	Finger to nose	Arm outstretched
Flexion/Extension	0.4 N m	0.2 N m
Adduction/Abduction	1.1 N m	0.5 N m

the required resistance force produced by the damper would be approximately 37 N. Given that the frequency of tremorous movement in the arm typically ranges between 3 and 12 Hz, the undamped velocity at the damper connection is projected at approximately 0.5–2.0 m/s. The primary variables that affect

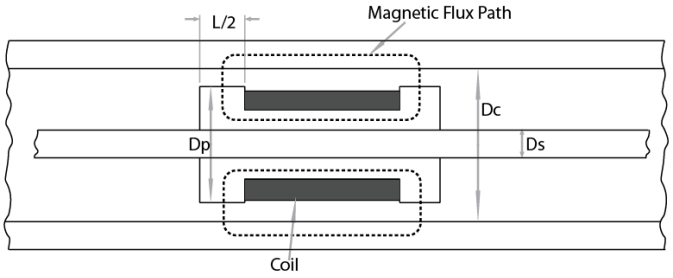

Fig. 2. Cross section diagram of a piston/cylinder magnetorheological damper design

the resistance force in this piston/cylinder design are the shaft diameter (Ds), piston diameter (Dp), cylinder inside diameter (Dc), active length (L), and the fluid's viscosity and yield strength (the latter being dependent upon the generated magnetic field and thus upon the dimensions of the coil and the applied current). A non-magnetic hollow shaft, to accommodate coil leads, 4.76 mm in diameter was employed to insure structural rigidity. The cylinder inside diameter was restricted to a maximum of 12.7 mm to keep the device's profile reasonably small. In order to minimize resistance of the damper in passive mode, a low-viscosity MR fluid was selected for the project (LORD MRF-122EG, $\mu = 0.042 \pm 0.020$ Pa.s). A relatively large piston/cylinder gap, 0.635 mm, was selected in order to reduce the damping rate in passive mode, thus defining the piston diameter at 11.43 mm. It was estimated that the coil could generate a magnetic flux density of 1.7 T at its core when the maximum admissible current of 0.54 A is applied. According to the manufacturer's specifications the required MR fluid yield strength of 15 kPa can be produced using a relatively small fraction of the maximum field intensity. Thus, the remaining design parameter (the active length of the piston) was determined from the mathematical model, requiring the damper to produce a resistance force of 37 N at an operating velocity of 0.5 m/s, when maximum current is applied to the coil. By regulating the current, then, the resistance force of the damper can be varied in real time to suit the patient's needs. The constructed damper weighs approximately 204 g. When run continuously with the maximum allowable current applied to its coil, the damper requires a 1.9 W power supply.

IV. Mathematical Model

Kamath, Hurt, and Wereley described a model of Bingham plastic flow that accounts for both the moving elements and the axial symmetry of a piston/cylinder device [19]. The Navier-Stokes equation, in cylindrical coordinates, is used to model the force equilibrium.

$$\rho\frac{\partial u}{\partial t} + \frac{\partial \tau}{\partial r} + \frac{\tau}{r} = \frac{\partial p}{\partial z} \tag{1}$$

Neglecting inertia and assuming a constant pressure gradient over the characteristic length, L,

$$\frac{\partial \tau}{\partial r} + \frac{\tau}{r} = \frac{\Delta P}{L}. \tag{2}$$

The flow in the annular gap is divided into two "post-yield" regions, where the shear stress exceeds the yield point of the Bingham plastic, and one "core flow" region, where it does not. This produces a velocity profile in the gap as shown in Fig. 3. Applying Bingham's description in the post-yield

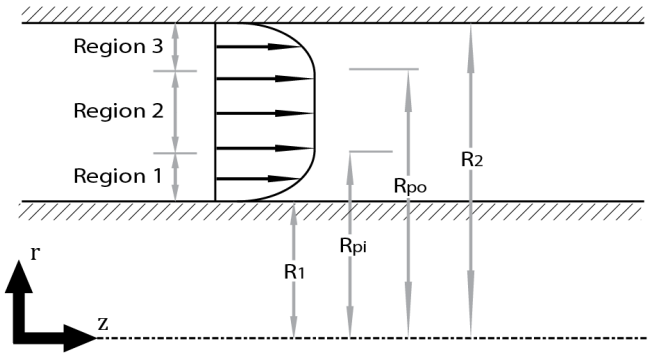

Fig. 3. Approximate velocity profile for a Bingham plastic in annular flow

region adjacent to the piston, where shear stress exceeds the yield stress of the fluid,

$$\tau = \tau_y + \eta\frac{du}{dr}, \tag{3}$$

$$\frac{d\tau}{dr} = \eta\frac{d^2u}{dr^2} \tag{4}$$

The force balance becomes

$$\eta\frac{d^2u}{dr^2} + (\tau_y + \eta\frac{du}{dr})/r = \frac{\Delta P}{L}. \tag{5}$$

Integration leads to the velocity profile in region 1,

$$u_1(r) = \frac{\Delta P}{4\eta L}r^2 - \frac{\tau_y}{\eta}r + C_1\ln(r) + C_2. \tag{6}$$

The post-yield region adjacent to the cylinder surface, region 3, requires a slightly different description:

$$\tau = -\tau_y + \eta\frac{du}{dr} \tag{7}$$

$$\frac{d\tau}{dr} = \eta\frac{d^2u}{dr^2} \tag{8}$$

$$\eta\frac{d^2u}{dr^2} + (-\tau_y + \eta\frac{du}{dr})/r = \frac{\Delta P}{L} \tag{9}$$

$$u_3(r) = \frac{\Delta P}{4\eta L}r^2 + \frac{\tau_y}{\eta}r + C_3\ln(r) + C_4 \tag{10}$$

The constants C_1, C_2, C_3, and C_4 can be determined by applying the following boundary conditions, assuming no-slip conditions at the cylinder wall and the moving piston head (the velocity of which is $-v_0$):

$$u_1(R_1) = -v_0 \qquad \frac{du_1}{dr}\,|_{r\to R_{pi}} = 0$$

$$u_3(R_2) = 0 \qquad \frac{du_3}{dr}\,|_{r\to R_{po}} = 0$$

In region 2, the velocity is uniform and defined by

$$u_2 = u_1(R_{pi}) = u_3(R_{po}). \tag{11}$$

A volume balance can thus be established, equating flow through the annular gap with fluid displacement due to the motion of the piston profile,

$$-v_0\pi(R_1^2 - R_s^2) = \int_{R_1}^{R_{pi}} u_1 2\pi r dr + u_2\pi(R_{po}^2 - R_{pi}^2) + \\ + \int_{R_{po}}^{R_2} u_3 2\pi r dr. \quad (12)$$

The system has effectively three equations with four unknowns, ΔP, R_{pi}, R_{po}, and u_2. To get the final equation necessary for a solution, the simplified Navier Stokes equation is integrated.

$$\frac{d\tau}{dr} + \frac{\tau}{r} = \frac{\Delta P}{L}$$

$$\tau(r) = \frac{\Delta P}{2L} r + \frac{C_5}{r} \quad (13)$$

$$r\tau(r) = \frac{\Delta P}{2L} r^2 + C_5 \quad (14)$$

The shear stress is known at the limits of the core flow region, allowing the boundary conditions,

$$\tau(R_{pi}) = \tau_y \qquad \tau(R_{po}) = -\tau_y$$

Substitution leads to the fourth necessary equation:

$$R_{pi}\tau_y = \frac{\Delta P}{2L} R_{pi}^2 + C_5 \quad (15)$$

$$-R_{po}\tau_y = \frac{\Delta P}{2L} R_{po}^2 + C_5 \quad (16)$$

$$(R_{pi} + R_{po})\tau_y = \frac{\Delta P}{2L}(R_{pi}^2 - R_{po}^2) \quad (17)$$

$$\tau_y = \frac{\Delta P}{2L}(R_{pi} - R_{po}) \quad (18)$$

Thus a complete, nonlinear model for estimation of the steady-state response of a piston/cylinder type damper with given dimensions is obtained.

V. Experimental Validation

A. Quasi-static Response

The experimental setup built to evaluate the properties of the small-scale MR damper included a disk with inertial loads actuated by a brushless DC electrical motor and corresponding amplifier (EDC, Cambridge, MA). An optical encoder (ACCU-Coder 260 N-T-02-S-1000, Encoder Products Co., Sandpoint, ID) was used measures the angular position of the disk. The MR damper was mounted in a rotating support and connected to the disk through a force transducer (MLP-50, Transducer Techniques, Temecula, CA). A multifunction RIO NI PCI-7833R FPGA card was employed for real-time data acquisition from the encoder and force sensor, and to control the electrical motor. In order to mitigate the discrete nature of the optical encoder readout, the angular velocity and acceleration were estimated in real time using a custom-developed algorithm implemented in the internal memory of the FPGA card. Static properties of the damper were measured by applying a slowly increasing linear force at the MRD's rod with constant current applied to the coil, and measuring the position change to determine the point of yield (see Fig. 5).

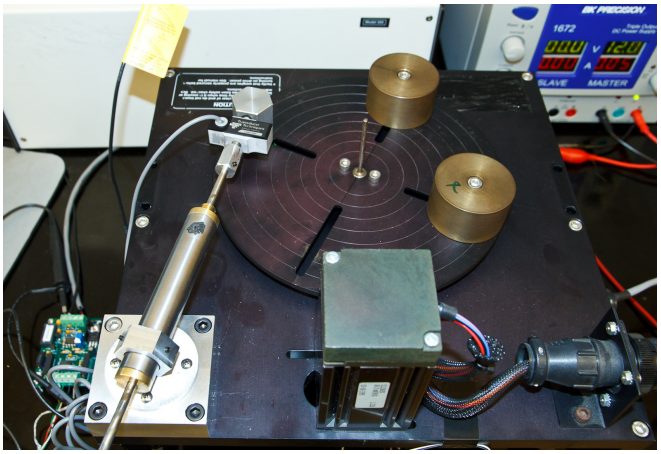

Fig. 4. Experimental setup for damper characterization

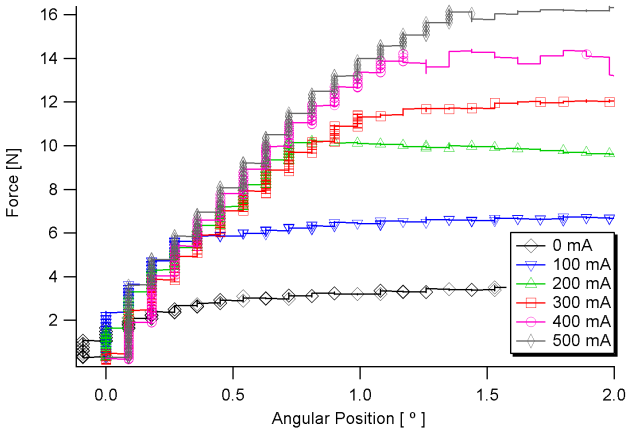

Fig. 5. Experimental values for the static resistance force of the damper at various applied currents

The mathematical model was used to determine the theoretical yield force corresponding to the experimental conditions. These theoretical values were given a bias of 3 N to account for friction in the seals and a gain of 0.10 to account for losses in the magnetic field. Good agreement was observed between measured and theoretical values for several applied currents as shown in Fig. 6.

B. Dynamic Response

The properties of the damper under dynamic magnetic fields were evaluated in an experimental setup that included the aforementioned force transducer, a linear stage (Parker 506042ETESD, Parker Hannifin, Cleveland, OH) actuated by a DC stepper motor (Zeta57-83, Parker Hannifin, Cleveland, OH). Step and haversine signals produced by a function generator (AFG 3201B, Tektronix, Beaverton, OR) were applied to the coil using a custom high frequency power amplifier, while an uniform motion was applied to the rod using the linear stage ($v = 25$ mm/s). Figure 7 shows the time dependence of the resistance force produced by the MRD, when step signals with 400 mA amplitude and positive and negative slope were applied to the coil. The resistance force produced

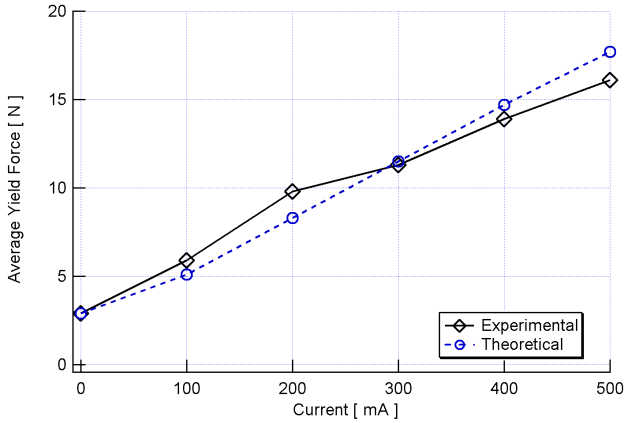

Fig. 6. Theoretical and experimental yield force versus applied coil current

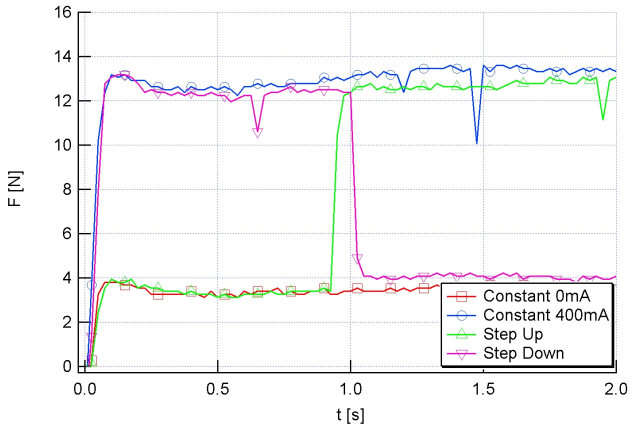

Fig. 7. Positive and negative step response compared to the resistance force produced by the damper at constant current

with the equivalent constant currents is shown for comparison. The 10–90% rise time was estimated at less than 0.05 s for both the positive and negative slope signals, supporting the suitability of the MRD for dynamic applications. Next, a series

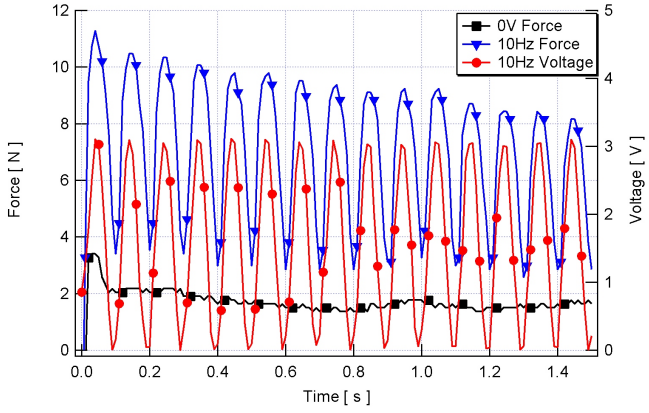

Fig. 8. Resistance force of the damper with a 10 Hz haversine function applied to the coil

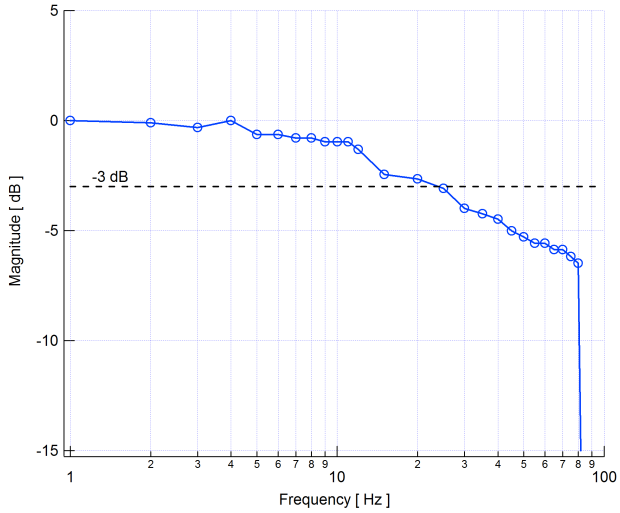

Fig. 9. Body diagram for the magnitude of the MRD' response to haversine signals

of experiments were conducted in which a haversine signal with 500 mA amplitude and specified frequency was applied to the coil, as the rod of the MRD was moved with a constant velocity of 25 mm/s on the linear stage. The resistance force created by the MRD was recorded for frequencies in the 1–100 Hz range, as seen in Fig. 8 for the 10 Hz experiment. Figure 9 shows the Body diagram of the magnitude of the response of the MRD to haversine inputs. Note the abrupt drop in the response at frequencies above 80 Hz. Using the -3 dB criterion, the damper bandwidth was estimated at 25 Hz. Since the majority of tremor disorders are characterized by frequencies as ranging between 3–12 Hz, the bandwidth of the damper is deemed sufficiently large for potential application in active control tremor suppression devices.

VI. Finite Element Analysis

The experimental measurements show that the theoretical model overestimates the resistance force produced by the MRD. To elucidate this discrepancy, finite element analysis of the magnetic field created in the piston/cylinder gap was performed using COMSOL Multiphysics (COMSOL Inc., Los Angeles, CA). Analysis of the constructed damper is shown in Fig. 10, the y-axis being the radial axis of symmetry. Fairly uniform field intensity is observed in the active portion of the fluid (the portion of fluid in the gap that is not directly adjacent to the coil), though the intensity is notably lower than that calculated in the electromagnet's core. The average field intensity was calculated over the active fluid volume, and this value was compared to the material data sheet to determine the expected yield stress of the fluid as a Bingham plastic.

Based on the projected yield stresses, the damper's static resistance forces were recalculated with the mathematical model. The measured values are presented alongside these expected values in Fig. 11. The force values are given the same bias applied previously to account for friction in the seals, but good agreement is observed with no correction factor.

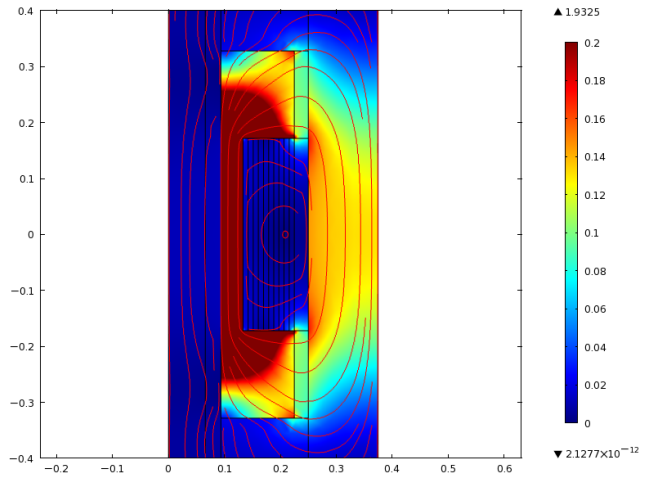

Fig. 10. Magnetic field intensity and flux lines of the constructed damper

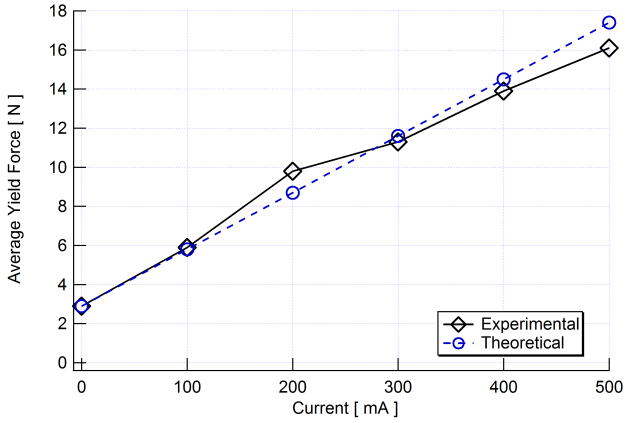

Fig. 11. Theoretical and experimental yield forces versus applied coil current, revised according to the finite element model

VII. Discussion and Conclusions

A small-scale MRD, dimensionally optimized for upper limb tremor suppression orthoses, was designed and constructed based on a mathematical model of MR fluid flow under magnetic field. Experimental validation of the model was conducted. As expected, modulating the magnetic field produced by the coil is shown to significantly alter the resistance force produced by the damper. Good agreement was observed between the values predicted by the theory and the measured force when friction and losses in the coil's magnetic field were considered.

Additionally, dynamic response of the damper was measured using time-dependent voltage signals applied to its coil. High fidelity was observed between input signal and output resistance force within the frequency range of tremorous motion described in the literature. Thus the bandwidth of the damper is deemed sufficiently large to merit potential application in a real-time tremor suppression strategy.

Finite element analysis was performed to model the distribution of the magnetic field within the piston/cylinder gap of the constructed damper, and high fidelity was shown between the experimentally observed resistance forces and those predicted with the mathematical model using this information.

The mathematical model presented in this paper assumed fully-developed flow within the damper, and fluid inertia was not taken into account. The model is therefore suitable to predict the operational range of the damper, but it is inadequate to accurately predict behavior in oscillatory flow, which would be seen in application to tremor reduction. In order to develop an effective control strategy for the attenuation of tremor with MR dampers, further modeling (e.g. taking fluid inertia and response time into account) is necessary.

References

[1] J. Benito-Len and E. D. Louis, "Essential tremor: emerging views of a common disorder." *Nat Clin Pract Neurol*, vol. 2, no. 12, pp. 666–78; quiz 2p following 691, Dec 2006. [Online]. Available: http://dx.doi.org/10.1038/ncpneuro0347

[2] G. Deuschl, P. Bain, and M. Brin, "Consensus statement of the movement disorder society on tremor," *Movement Disorders*, vol. 13, no. 3, pp. 2–23, 1998.

[3] D. Sirisena and D. Williams, "My hands shake: Classification and treatment of tremor," *Australian Family Physician*, vol. 38, no. 9, pp. 678–683, 2009.

[4] Y. Katayama, T. Kano, K. Kobayashi, H. Oshima, C. Fukaya, and T. Yamamoto, "Difference in surgical strategies between thalamotomy and thalamic deep brain stimulation for tremor control," *Journal of Neurology*, vol. 252, no. 4, pp. 17–22, 2005.

[5] E. Flora, C. Perera, A. Cameron, and G. Maddern, "Deep brain stimulation for essential tremor: A systematic review," *Movement Disorders*, vol. 25, no. 11, pp. 1550–1559, 2010.

[6] J. Sanes, P. LeWitt, and K. Mauritz, "Visual and mechanical control of postural and kinetic tremor in cerebellar system disorders," *Journal of Neurology, Neurosurgery, and Psychiatry*, vol. 51, no. 7, pp. 934–943, 1988.

[7] M. Aisen, A. Arnold, I. Baiges, S. Maxwell, and M. Rosen, "The effect of mechanical damping loads on disabling action tremor," *Neurology*, vol. 43, no. 7, pp. 1346–1350, 1988.

[8] J. Kotovsky and M. Rosen, "A wearable tremor-suppression orthosis," *Journal of Rehabilitation Research and Development*, vol. 35, no. 4, pp. 373–387, 1998.

[9] R. Loureiro, J. Belda-Lois, E. Lima, J. Pons, J. Sanchez-Lacuesta, and W. Harwin, "Upper limb tremor suppression in adl via and orthosis incorporating a controllable double viscous beam actuator," Chicago, 2005, pp. 119–122.

[10] J. Belda-Lois, A. Page, and J. Baydal-Bertomeu, *Rehabilitation Robotics: Biomechanical Constraints in the Design of Robotic Systems for Tremor Suppression*. Vienna: I-Tech Education and Publishing, 2007.

[11] M. Manto, M. Topping, M. Soede, J. Sanchez-Lacuesta, W. Harwin, J. Pons, J. Williams, S. Skaarup, and L. Normie, "Dynamically responsive intervention for tremor suppression," *Rehabilitation Robotics*, vol. 22, no. 3, pp. 120–132, 2003.

[12] E. Rocon, M. Manto, J. Pons, S. Camut, and J. Belda, "Mechanical suppression of essential tremor," *The Cerebellum*, vol. 6, no. 1, pp. 73–78, 2007.

[13] E. Rocon, J. Belda-Lois, A. Ruiz, M. Manto, J. Moreno, and J. Pons, "Design and validation of a rehabilitation robotic exoskeleton for tremor assessment and suppression," *IEEE Transactions on Neural Systems and Rehabilitation Engineering*, vol. 15, no. 3, pp. 367–378, 2007.

[14] E. Rocon, A. Ruiz, and J. Pons, "Rehabilitation robotics: a wearable exo-skeleton for tremor assessment and suppression," Barcelona, 2005, pp. 2271–2276.

[15] E. Rocon, M. Manto, J. Pons, J. Belda, and S. Camut, "Evaluation of a wearable orthosis and an associated algorithm for tremor suppression," *Physiological Measurement*, vol. 28, no. 4, pp. 415–425, 2007.

[16] J. Rosen, S. Burns, and J. Perry, "Upper-limb powered exoskeleton design," *IEEE/ASME Transactions on Mechatronics*, vol. 12, no. 4, pp. 408–417, 2007.

[17] H. Gurocak and J. Blake, "Haptic glove with mr brakes for virtual reality," *IEEE/ASME Transactions on Mechatronics*, vol. 14, no. 5, pp. 606–615, 2009.

[18] M. Kermani and A. Shafer, "On the feasibility and suitability of mr fluid clutches in human-friendly manipulators," *IEEE/ASME Transactions on Mechatronics*.

[19] G. Kamath, M. Hurt, and N. Wereley, "Analysis and testing of bingham plastic behavior in semi-active electrorheological fluid dampers," *Smart Materials and Structures*, vol. 5, no. 5, pp. 576–590, 1996.